Study on the correlation between Solid Oxide Fuel Cell Ni-YSZ anode performance and reduction temperature

Zhenjun Jiao[1], Ai Ueno[2] and Naoki Shikazono[1]

1. Institute of Industrial Science, The University of Tokyo, 4-6-1 Komaba, Meguro-ku, Tokyo 153-8505, Japan
2. Department of Mechanical Engineering, The University of Tokyo, 7-3-1 Hongo, Bunkyo-ku, Tokyo 113-8656, Japan

E-mail: zhenjun@iis.u-tokyo.ac.jp

Abstract. The influences of reduction temperature on the initial performance and short-time durability of nickel-yttria-stabilized zirconia composite solid oxide fuel cell anode were investigated. Anode microstructures before and after operation were quantitatively analyzed by three-dimensional reconstruction based on focused ion beam-scanning electron microscopy technique. The anode reduced at 500 ^{o}C showed the worst initial performance and stability in operation and the anode reduced at 800 ^{o}C showed the smallest polarization resistance. The anode reduced at 1000 ^{o}C showed the most stable performance with polarization resistance enhanced with operation. It is found that higher reduction temperature leads to dense nickel and enhances nickel-yttria-stabilized-zirconia interfacial bonding, which can inhibit nickel sintering and improve the composite anode stability in long-time operation.

Keywords: SOFC, anode, TPB, Reduction temperature

1. Introduction

Solid oxide fuel cell (SOFC, hereafter), as a high efficiency and fuel flexibility energy conversion device, has been attracting more and more attentions in recent decades [1], while long time operation stability of SOFC electrodes remain as one of the main challenges. For the nickel-yttria-stabilized-zirconia (Ni-YSZ, hereafter) anodes, major anode degradation mechanism is attributed to the agglomeration of Ni phase, especially during the initial operation period ($<$ 200 hours). It has been reported that this initial agglomeration is associated with the initial fast sintering kinetics of Ni [2]. Ni sintering results in the reduction of active three phase boundary (TPB, hereafter) density and Ni network connectivity. The sintering mechanism depend on many process factors, such as, sintering temperature, fuel humidity and contaminants [3, 4]. A few investigations were conducted to investigate the influence of reduction temperature on the pure initial Ni particle microstructure. Plascencia & Utigard [5] and Utigard et al. [6] have studied the reduction process of NiO particles at different temperatures. It is shown that different initial reduction temperatures lead to totally different morphologies of Ni particles in millimeter-scale. Thus, for conventional composite anode, the corresponding initial performance and durability can be also influenced by the Ni morphological differences created during the reduction process.

Several researchers have reported on the influence of reduction temperature on the initial Ni-YSZ microstructures [7, 8, 9]. Jeangros et al. [7, 8] have observed NiO reduction process of NiO-YSZ composite anode in-situ in an environmental transmission-electron-microscopy at low temperature. It is reported that the reduction of NiO starts from 380 ^{o}C at NiO-YSZ interface in a composite anode with very low hydrogen pressure. Zhu et. al. [10] have reported that the initial microstructure of Ni-YSZ and the corresponding anode performances can be controlled by reduction and sintering processes of NiO to Ni. A model was proposed to qualitatively describe the reducing and sintering mechanisms and combined effects on anode microstructure changes at different initial reduction temperatures. However, no further quantitative investigation was conducted to support the model and the experimental results. Recently, three-dimensional (3D, hereafter) reconstructions of SOFC electrodes have been carried out by applying focused ion beam scanning electron microscopy (FIB-SEM) technique [11, 12, 13, 14]. This method provides quantitative information of composite cermet microstructure, such as active TPB density, phase percolation etc., which are strongly correlated to the electrode performance.

2. Experimental

2.1. Cell preparation

Electrolyte-supported cells were used in this study. The anode cermet powder was prepared by mechanically mixed NiO and YSZ powders (AGC Seimi Chem. Corp., Japan) for 48 hours, where the volume ratio of NiO to YSZ was 60% : 40 %. The solid mixture was then mixed with terpineol solvent and the ethylcellulose binder in agate mortar to obtain anode slurry. The slurry was screen-printed onto commercial dense 8 mol % YSZ pellet (diameter 30 mm, thickness 0.5 mm, Toso Nikkemi Corp., Japan) with a diameter of 10 mm. Anodes were sintered at 1450 ^{o}C for 3 hours. The anode thickness was measured to be about 30 microns after sintering. The cathode material was prepared by mixing $(La_{0.8}Sr_{0.2})_{0.97}MnO_3$ (LSM, hereafter) powder with YSZ powder in a mass ratio of 50% : 50 %. The cathode slurry was screen-printed onto the counter side of the pellet with a diameter of 10 mm and sintered at 1200 ^{o}C for 2 hours.

2.2. Electrochemical evaluation

The reduction of anode was conducted by introducing 5 % hydrogen for the initial half of the reduction time and pure hydrogen for the other half subsequently to ensure full reduction of Ni phase. Three anodes were reduced at 500 ^{o}C, 800 ^{o}C and 1000 ^{o}C for 120 minutes, 40 minutes and 15 minutes, respectively. The performances of anodes were then measured at 800 ^{o}C with 3 %H_2O humidified hydrogen as a fuel and pure oxygen as an oxidant (gas flow rates are 100 mlmin^{-1} for both anode and cathode). Electrochemical impedance spectroscopy (frequency range: $1 - 10^5$ Hz, AC signal strength: 10 mV) measurements were conducted using Solatron frequency analyzer (1255WB) at open circuit voltage (OCV, hereafter).

2.3. FIB-SEM observation

The anodes after experiments were then analyzed by FIB-SEM (Carl Zeiss, NVision 40). The samples were first infiltrated by low viscosity epoxy resin under low pressure atmosphere (ca. 15 Pa), so that the pores of the porous electrode could be easily distinguished during FIB-SEM observation. The details of dual-beam FIB-SEM observation technique are introduced in Refs. [11, 14].

3. Results and Discussions

3.1. Electrochemical evaluation experiment results

The anodes reduced at different temperatures were operated with a current density of 200 mAcm^{-2} for 100 hours to investigate the initial performances and durabilities. Figure 1 shows the time variation of anode-to-reference (A-R, hereafter) terminal voltage for three anodes. It is seen that a relatively high degradation rate can be observed for the anode reduced at 500 ^{o}C and its performance became very unstable after about 45 hours in operation. For the anode reduced at 800 ^{o}C, degradation rate decreased with time and the performance tended to enter a stable stage with the proceeding of operation. For the anode reduced at 1000 ^{o}C, the performance of anode was enhanced in the initial 10 hours and showed similar degradation process as the one reduced at 800 ^{o}C in the rest of the operation.

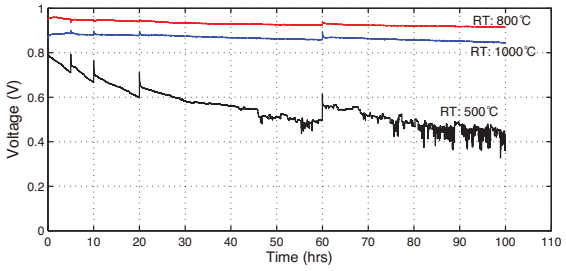

Figure 1. Anode-reference terminal voltage against time measured with different reduction temperatures by galvanostatic method for 100 hours with a current density of 0.2 Acm^{-2}.

The A-R impedance spectra against time for three anodes are shown in Fig. 2 [3]. The anode reduced at 500 ^{o}C showed the largest initial A-R ohmic and polarization resistances. The polarization resistances of anodes reduced at 500 ^{o}C and 800 ^{o}C experienced continuous degradation while for the anode reduced at 1000 ^{o}C, the polarization resistance decreased continuously in operation. It is seen that anode reduced at 1000 ^{o}C showed the most stable performance during the operation process.

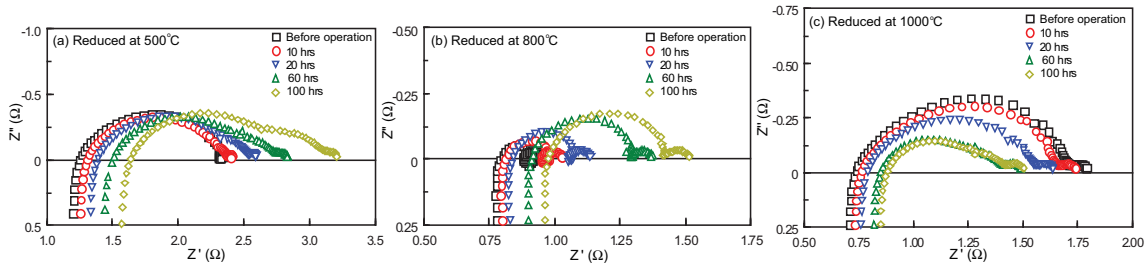

Figure 2. Comparison of A-R impedance spectra evolution in OCV against time within 3 % H_2O hydrogen of anodes reduced at (a) 500^{o}C, (b) 800^{o}C and 1000^{o}C.

3.2. Microstructure analysis

Figures 3 (a)-(c) and 4 (a)-(c) show the 2D SEM images for the FIB-polished cross-sections of Ni-YSZ anodes before and after the 100 hours operation, respectively. White, gray and black regions correspond to Ni, YSZ and pore, respectively. When anode was reduced at 500 ^{o}C, open closed pores can be observed uniformly distributed in Ni phase right before the operation, while most of the closed pores disappeared after 100 hours operation with Ni particle became round, which can be attributed to Ni sintering. For the anodes reduced at 800 ^{o}C and 1000 ^{o}C,

relatively dense Ni particles can be observed both before and after operation without obvious shape change. YSZ particle was not obviously influenced by the reduction temperature. The 3D microstructures of composite Ni-YSZ anodes reduced at 500 ^{o}C, 800 ^{o}C and 1000 ^{o}C before and after the 100 hours operation are shown in Figures 3 (d)-(f) and 4 (d)-(f). Ni and YSZ phases are demonstrated as gray and green colors, respectively. It can be seen that the anode reduced at 500 ^{o}C experienced obvious morphological change for Ni particle. On the other hand, Ni phase in anodes reduced at 800 ^{o}C and 1000 ^{o}C experienced no obvious morphological change.

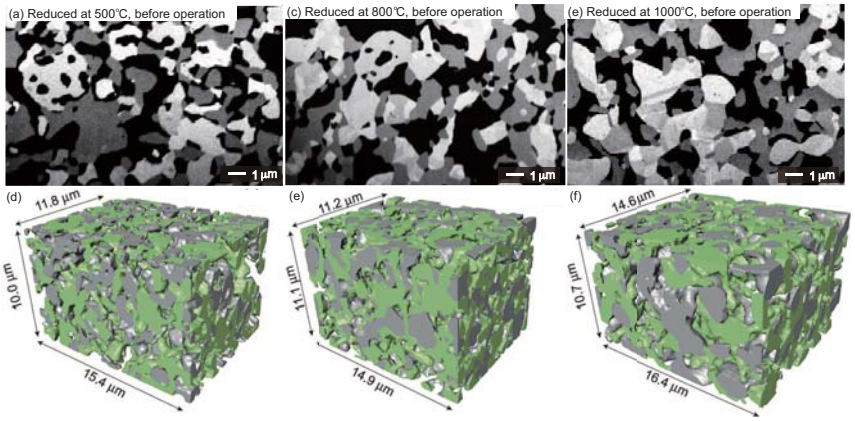

Figure 3. SEM cross-sectional images (White: Ni, gray: YSZ, and black: Pore) and the corresponding 3D reconstructions (Gray: Ni and green: YSZ) of anodes after reduction at (a) 500^{o}C, (b) 800^{o}C and (c) 1000^{o}C within 3 % H_2O hydrogen.

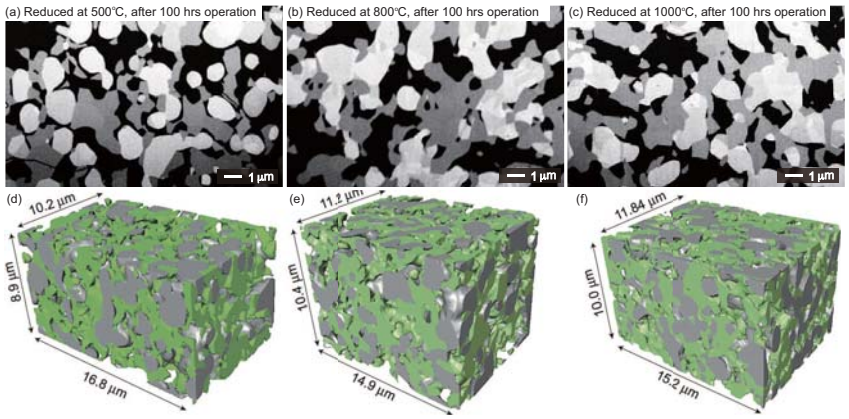

Figure 4. SEM cross-sectional images (White: Ni, gray: YSZ, and black: Pore) and the corresponding 3D reconstructions (Gray: Ni and green: YSZ) of anodes reduced at (a) 500^{o}C, (b) 800^{o}C and (c) 1000^{o}C after 100 hours operation within 3 % H_2O hydrogen at 800^{o}C with a current density of 200 mAcm^{-2}.

In order to quantitatively investigate the anode microstructural changes before and after operation, the specific interface areas and total and active TPB densities are summarized in Figs. 5. It is seen that the specific Ni-YSZ interface area decreased after the operations for anodes reduced at 500 ^{o}C and 800 ^{o}C but increased for the one reduced at 1000 ^{o}C. Anode reduced

at 500 ^{o}C showed the smallest specific Ni-YSZ interface area both before and after operation, which indicates its weakest Ni-YSZ interfacial bonding. At the same time the largest specific Ni-pore interface area can be attributed to the highly porous Ni, which promoted the sintering of Ni in operation. Specific Ni-pore interface areas decreased in operation for anodes reduced in all three temperatures, which can be explained by Ni sintering driven by the reduction of surface free energy in three cases. For TPB densities, it is seen that the anode reduced at 800 ^{o}C showed the largest total and active TPB densities before operation while the anode reduced at 1000 ^{o}C showed the smallest ones. In operation, the anode reduced at 500 ^{o}C showed the largest degradation rates for both total and active TPB densities. After operation, anode reduced at 1000 ^{o}C showed the largest total and active TPB densities comparing two the other two anodes.

It is well known that active TPB density in Ni-YSZ anode strongly affect its electrochemical

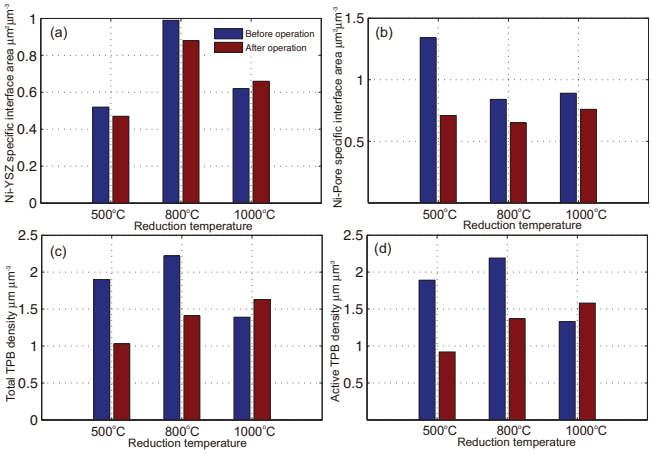

Figure 5. (a)(b) Specific interface area and (c)(d) TPB densities before and after operation for anodes reduced at 500 ^{o}C, 800 ^{o}C and 1000 ^{o}C.

performance, i.e. both ohmic and polarization resistances [15, 16]. As shown in Fig. 5 (d), anode reduced at 800 ^{o}C showed the largest initial active TPB density, which is corresponding to the smallest polarization resistance after reduction. The enhancement of active TPB densities for anode reduced at 1000 ^{o}C thus explains the decrease of polarization resistance in operation. However, anode reduced at 500 ^{o}C did not show the smallest initial active TPB densitiy, which can not explain the corresponding largest ohmic and polarization resistances as shown in Fig. 2. After 100 hours operation, the anode reduced at 500 ^{o}C showed the lowest active TPB density which explained the largest polarization resistance while the active TPB densities of anodes reduced at 800 ^{o}C and 1000 ^{o}C can not explain the corresponding polarization resistances sequence. It seems that current active TPB density can not be used as the only parameter to predict anode performance.

For ohmic resistance, it is well known that the A-R ohmic resistance is determined by the ionic resistivity of YSZ, the electronic resistivity of Ni and any possible contact resistance at Ni-YSZ interface [1]. Butz et al. [17] have reported that Ni can diffuse quickly at commonly applied sintering temperatures into 8 mol% Y_2O_3-Zirconia phase. During the reduction of NiO to metallic Ni, which has a much lower solubility in YSZ, the excess Ni can be exsolved from YSZ and accelerates the appearance of fine tetragonal phase. The conductivity of YSZ thus can be affected by the cubic-tetragonal-crystal transformation which irreversibly reduces the YSZ ionic conductivity [18, 19, 20]. However, without long-time operation, the decrease of YSZ ionic conductivity can not cause very large degradation on A-R ohmic resistance. Besides the

influence of YSZ ionic conductivity, the reduction of active TPB density partially contributes to the increase of ohmic resistance due to the concentration of the ionic current paths at Ni-YSZ interface [1, 3, 21]. However, for anode reduced at 1000 ^{o}C, the smallest initial ohmic resistance shown in Fig. 2 can not be explained by the corresponding smallest active TPB density as shown in Fig. 5 (d), which also supports the assumption that anode performance can not just be predicted by the active TPB density based on FIB-SEM reconstruction without considering about Ni-YSZ interface. Compared to the other two reduction temperatures, the very large ohmic resistance of anode reduced at 500 ^{o}C can only be explained by the possible contact resistance at Ni-YSZ interface.

Based on the current FIB-SEM technique, the micro-scale reconstruction may not be enough to describe the actually TPB length precisely to predict the anode performance. In sub-micron-scale, Ni-YSZ interface was found to show complicate microstructure which may generate extra active TPB length that can not be described by the current 3D reconstructions [22]. Thus, not just active TPB density, specific Ni-YSZ interface area should also be considered to predict the anode performance. Thus, although anode reduced at 1000 ^{o}C showed the smallest initial active TPB density, the corresponding specific Ni-YSZ interface area was found to be the largest among the three reduction temperatures. On the other hand, anode reduced at 500 ^{o}C showed the second smallest initial active TPB density while its specific Ni-YSZ interface area was the smallest. Consider about the contribution of specific Ni-YSZ area on anode performance, it makes sense that anode reduced at 500 ^{o}C showed the largest initial polarization resistances while the anode reduced at 1000 ^{o}C did not. The very small specific Ni-YSZ interface area of anode reduced at 500 ^{o}C may also explain its instability of performance in operation with a weak Ni-YSZ interfacial bonding.

In order to further study the process of anode reduction at different temperatures, a 800 nm-thick Ni-film electrode was fabricated by Ni sputtering method (CANON-ANELVA E-200S, 1 Pa, 300 W), with an area of 1.0 cm^2, on YSZ pellet. The Ni-film anodes were then sintered at 1450 ^{o}C for 3 hours to produce NiO film and then reduced at 500 ^{o}C, 800 ^{o}C and 1000 ^{o}C in diluted hydrogen as composite anode. The corresponding cross-sectional SEM images of Ni-YSZ interfaces reduced at different temperatures and kept at 800 ^{o}C in 3 % humidified hydrogen for 100 hours are shown in Fig. 6. In the reduction process at 500 ^{o}C, Ni became full of sub-micron pores after reduction as shown in Fig. 6 (a) and Ni-YSZ interfacial bonding was destructed by the gaps formed before operation. The Ni sintering can be highly promoted by the sub-micron pores and result in a very fast morphological change of Ni in a very short time when the anode reduced at 500 ^{o}C was heated up to 800 ^{o}C for operation as shown in Fig. 3 (a). When Ni-film electrode was reduced at 800 ^{o}C, only part of Ni-YSZ interface lost contact after reduction. For the one reduced at 1000 ^{o}C, Ni was densified after reduction and remained contacting with YSZ surface tightly without gap.

In the reduction process of anode, the residual stresses formed in NiO-YSZ sintering can be released by the reorganization of Ni [5, 6]. Reduction at low temperature, such as at 500 ^{o}C, is dominated by volume reduction rather than Ni sintering. The solid volume reduction can be achieved by the formation of large amount of sub-micron inner pores. It has been reported that the reduction process at low temperature starts from the grain surface or boundary of NiO with relatively low binding energy [7, 8, 10], which explains the gaps formed at Ni-YSZ interface and inside Ni particle. During the temperature rise from 500 ^{o}C to 800 ^{o}C before operation, the closed pores coalesced and vanished due to Ni sintering as shown in Fig. 3 (a). In the reduction process at 800 ^{o}C, Ni sintering dominated the Ni morphological change with the closed pores coalesced and vanished. Certain larger closed pores formed in the coalescence

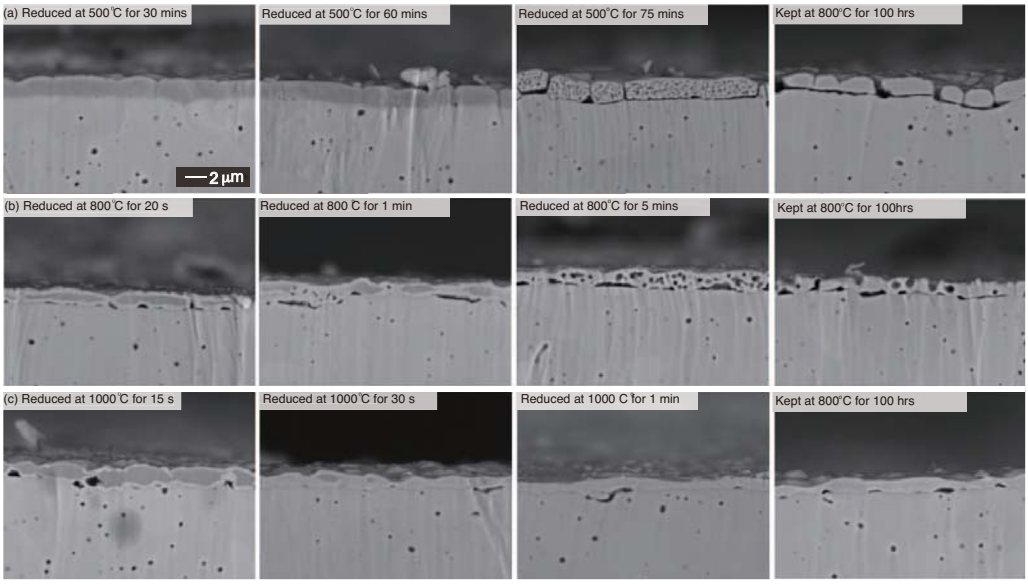

Figure 6. Cross-section SEM images of reduction process and kept at 800^{o}C for 100 hours for Ni-film anodes reduced at (a) 500^{o}C, (b) 800^{o}C and (c) 1000^{o}C within 5 % H_2 diluted by N_2 at different times.

of initial sub-micron pores remained inside Ni after reduction. Anode reduction at 1000 ^{o}C was dominated by Ni sintering and dense Ni particles can be formed as shown in Fig. 6 (c). It is seen that higher reaction temperature leads to the domination of Ni sintering mechanism in Ni morphological change and promotes the bonding between Ni and YSZ. The degradation rate of specific Ni-YSZ interface area supports the assumption that higher reduction temperature may enhance Ni-YSZ interfacial bonding.

After being kept for 100 hours at 800 ^{o}C in 3 % humidified hydrogen, it is seen that Ni film reduced at 500 ^{o}C delaminated from YSZ surface entirely, with dense Ni formed by sintering. Ni film reduced at 800 ^{o}C remained contact with YSZ surface with initial small inner pores after reduction merged into larger size ones. Ni film did not become dense after 100 hours because Ni sintering was constrained by Ni-YSZ interfacial bonding. Dense Ni film reduced at 1000 ^{o}C remained contact with YSZ surface tightly as after reduction without obvious change, which proves the strong Ni-YSZ interfacial bonding. It can be seen that compared to the other two reduction temperatures, reduction at 1000 ^{o}C leads to the strongest Ni-YSZ interfacial bonding in reduction process. The phenomena observed in all images were found uniformly distributed along Ni-YSZ interfaces. The assumption of enhanced Ni-YSZ interfacial bonding is thus supported by this experiment, which may explain the enhanced specific Ni-YSZ interface area and TPB density for composite anode reduced at 1000 ^{o}C as shown in Figs. 5.

4. Conclusion

Ni-YSZ composite anodes were reduced at 500 ^{o}C, 800 ^{o}C and 1000 ^{o}C and then operated at 800 ^{o}C for 100 hours in 3 %H_2O humidified hydrogen with time-dependent electrochemical performances measured. The microstructures after reduction and operation were quantitatively studied by FIB-SEM technique. The anode reduced at 800 ^{o}C showed the best initial performance which can be attributed to the largest active TPB density. The anode reduced at 1000 ^{o}C

showed the most stable performance during the operation while the anode reduced at 500 ^oC showed the largest degradation rate for both ohmic and polarization resistances which can be explained by the weak Ni-YSZ interfacial bonding and the enhanced Ni sintering caused by large amount of sub-micron closed pores formed in reduction process. It was seen that active TPB density measured based on micro-scale 3D reconstruction is not enough for predicting the anode performance without considering on specific Ni-YSZ interface area. It is found that reduction at 1000 ^oC leads to the improvement of anode stability in a long-time operation by forming enhanced Ni-YSZ interfacial bonding and dense Ni which can prohibit the sintering. Ni-film electrode was fabricated to prove that reduction temperature influenced the anode performance by changing Ni-YSZ bonding and Ni phase morphology. With the same initial microstructure, anode performance stability can be enhanced by increasing the reduction temperature.

Acknowledgments

This work was partly supported by the project of Core Research for Evolutional Science and Technology (CREST) under the Development of Technology on Solid Oxide Fuel Cell (SOFC) Project.

References

[1] C. S. Subhash and K. Kevin 2003 High Temperature Solid Oxide Fuel Cells: Fundamentals, Design and Applications, *Elsevier Advanced Technology*
[2] S. Koch and P. V. Hendriksen, M. Mogensen, Y-L. Liu, N. Dekker, B. Rietveld, B. De. Haart and F. Tietz 2006 *Fuel Cells*, **2**, 130-136
[3] Z. Jiao, G. Lee, N. Shikazono and N. Kasagi 2012 *J. Electrochem. Soc.* **159(7)**, F278-F286
[4] Z. Jiao, N. Shikazono and N. Kasagi 2012 *J. Electrochem. Soc.* **159 (3)**, B285-B291
[5] G. Plascencia and T. Utigard 2009 *Chem. Eng. Sci.* **64** 3879-3888
[6] T. Utigard, M. Wu, G. Plascencia and T. Marin 2005 *Chem. Eng. Sci.* **60** 2061-2068
[7] Q. Jeangros, T. W. Hansen, J. B. Wagner, C. D. Damsgaard, R. E. Dunin-Borkowski, C. Hebert and J. Van herle and A. Hessler-Wyser 2012 *J. Mater. Sci.* **48** 2893-2907
[8] Q. Jeangros, A. Faes, J. B. Wagner, T. W. Hansen, U. Aschauer, J. Van herle, A. Hessler-Wyser and R. E. Dunin-Borkowski 2010 *Acta. Materialia.* **58** 4578-4589
[9] M. Andrzejczuk, O. Vasylyev, I. Brodnikovskyi, V. Podhurska, B. Vasyliv, O. Ostash, M. Lewandowska and K. J. KurzydCowski 2014 *Mater. Charact.* **87** 159-165
[10] X. Zhu, C. Guan, Z. Lu and W. Su 2013 *J. Electrochem. Soc.* **160** F1170-F1174
[11] Jiao Z and Shikazono N 2010 *J. Power Sources* **24** 8019-8027
[12] Sumi H, Kishida R, Kim J K, Muroyama H, Matsui T and Eguchi K 2009 *J. Electrochem. Soc.* **157** B1747-B1752
[13] Matsui T, Kishida R, Kim J K, Muroyama H and Eguchi K 2010 *J. Electrochem. Soc.* **157** B776-B781
[14] Iwai H, Shikazono N, Matsui T, Teshima H, Kishimoto M, Kishida R, Hayashi D, Matsuzaki T, Kanno D, Saito M, Muroyama H, Eguchi K, Kasagi N and Yoshida H 2010 *J. Power Sources* **195** 955-961
[15] Fukui T, Ohara S, Naito M and Nogi K 2002 *J. Power Sources* **110** 91-95
[16] Thyden K 2008 Ph.D. Thesis, Riso National Laboratory for Sustainable Energy, Technical University of Denmark, Denmark.
[17] Butz B, Lefarth A, Stormer H, Utz A, Ivers-Tiffee E and Gerthsen D 2012 *Solid State Ionics* **214** 37-44
[18] Linderoth S, Bonanos N, Jensen K V and Bilde-Sorensen J B 2001 *J. Am. Ceram. Soc.* **84** 2652-2656
[19] Kuzjukevics A and Linderoth S 1997 *Solid State Ionics* **93** 255-261
[20] Fukui T, Ohara S and Nogi K 1998 *Electrochem. Solid St.* **1** 120-122
[21] Jiao Z, Takagi N, Shikazono N and Kasagi N 2011 *J. Power Sources* **196** 1019-1029
[22] Jiao Z, Takagi N, Shikazono N and Kasagi N 2011 *J. Power Sources* **196** 8366-8376